A Wideband Capacitively Fed Suspended Plate Antenna for Wearable Wireless Sensors

Mohammad Vatankhah Varnoosfaderani, David V.Thiel, Junwei Lu
School of Engineering
Griffith University
Brisbane, Australia
S2862672@griffithuni.edu.au

Abstract— **A suspended shorted patch capacitively fed using an inverted L-shape feed is a compact antenna for wearable wireless sensors. A short microstrip line was printed on the sensor PCB to connect the antenna to a transceiver chip. The shorting of the suspended patch was done using printed silver ink on the side wall of a 22mm x 6mm x 6mm block of polycarbonate plastic that suspends the mounted patch. Based on the required bandwidth, the height of the plastic block can be decreased to 2 mm. The simulated 10 dB bandwidth of the antenna, was 98% (2.2 GHz-6.44 GHz) for a 6 mm high polycarbonate block. The size of the sensor including the elevated antenna was 35mm x 22mm x 9mm. The antenna features an upward directional radiation pattern which decreases the electromagnetic coupling between the human body and the antenna. The simulated total radiation efficiency of antenna is more than 90% in free space which drops to 70% at 2.4 GHz and 80% at 5.8 GHz when the sensor is located next to a voxel model of the human body and simulated maximum gain of antenna was 2.3 dBi at 2.4 GHz, 3.5 dBi at 3.5 GHz and 4.6 dBi at 5.8 GHz respectively.**

Keywords— Capacitive feed, PIFA antenna, Wearable antenna, Wearable Wireless sensor, Wideband antenna, Shorted patch, Suspended Patch

I. INTRODUCTION

Developing a small and efficient antenna is one of the main challenges in designing wearable wireless sensors. Using small antenna structures such as meandered monopole or dipole antennas, which do not feature a full ground plane, causes a considerable amount of electromagnetic coupling between the antenna of the sensor and the human body. This leads to impedance mismatch on the antenna port and power absorption by body tissues which decrease the radiation efficiency of the wireless sensor [1]. Different techniques including substrate integrated waveguide (SIW) cavities [2], electromagnetic band gap (EBG) substrates [3], photonic band gap (PBG) structures [4], parasitic elements [1, 5] , and printed embedded slot antennas [6] have been used to decrease the electromagnetic coupling between body tissues and the antenna of the sensor. The main drawbacks of these methods are the large size and limited bandwidth. Griffith University has developed small wireless sensor nodes to monitor human movement in sport during both training and match play [7]. One device (z-core[8]) includes a standard design meander line monopole antenna and is housed in a robust rectangular waterproof plastic case. In [1], the performance of z-core on the human body was investigated by the authors. The results showed a huge drop in total radiation efficiency of the standard meandered monopole antenna of the sensor from 90% to 13% at 2.45 GHz after wearing the sensor on the arm of a human body. An external parasitic element was used by the authors to improve the radiation efficiency of the sensor by 13% [1], which is not large enough compared with the 78% loss after wearing the sensor on a human arm. A printed embedded slot antenna [6] was proposed by authors to be integrated on the internal walls of the sensor. This solution was not practical because of the complexity of manufacturing and the large size of the required wideband feed. Suspended patch structures can be a solution for this problem because they can be installed on a corner of the PCB of the sensor. They are widely used in UWB applications and are fed using different techniques either directly as structures presented in [9-14] or can be electromagnetically coupled to such as feeds used in [15-19]. The feed of the antenna in [14] was directly connected to the suspended patch and the longest current path is a loop including the feed that determines the lowest resonance frequency of the antenna. In [16] a vertical feed was used to couple to the shorted part of the patch. Capacitive fed suspended patch antennas [15] are wideband and feature a directional radiation pattern opposite to the ground plane which is desired in wearable wireless sensors. This structure was used in [19] with a capacitive load to design a mobile handset antenna. Easy manufacturing is another important criterion in designing antennas for wireless sensors to facilitate the mass production. Suspending the patch in the air [15, 19] or using parasitic elements as in [11, 14] is not easy to fabricate. In the case of capacitive coupling, the feed can be adjacent to the radiator as in [15, 18, 19] or to the shorting wall as in [16]. In this paper, the feed is electromagnetically coupled both to the suspended shorted patch using a small printed rectangle on the bottom layer of the suspended patch, and to the shorting wall through a printed silver ink on a block of polycarbonate. This simplifies the manufacturing process and maximizes the bandwidth. This design also can be used along with new 3D circuit printers for fast mass production of wireless sensors. The main advantage of this antenna is that it only needs a small microstrip feed line which fits on a small portion of the wireless sensor PCB and the rest of the space on the board can be used for other electronic components. The total height of the antenna, including substrate thicknesses, can be decreased to 4.6 mm, but the bandwidth will be limited to 12.2% (2.22 GHz-2.51 GHz).

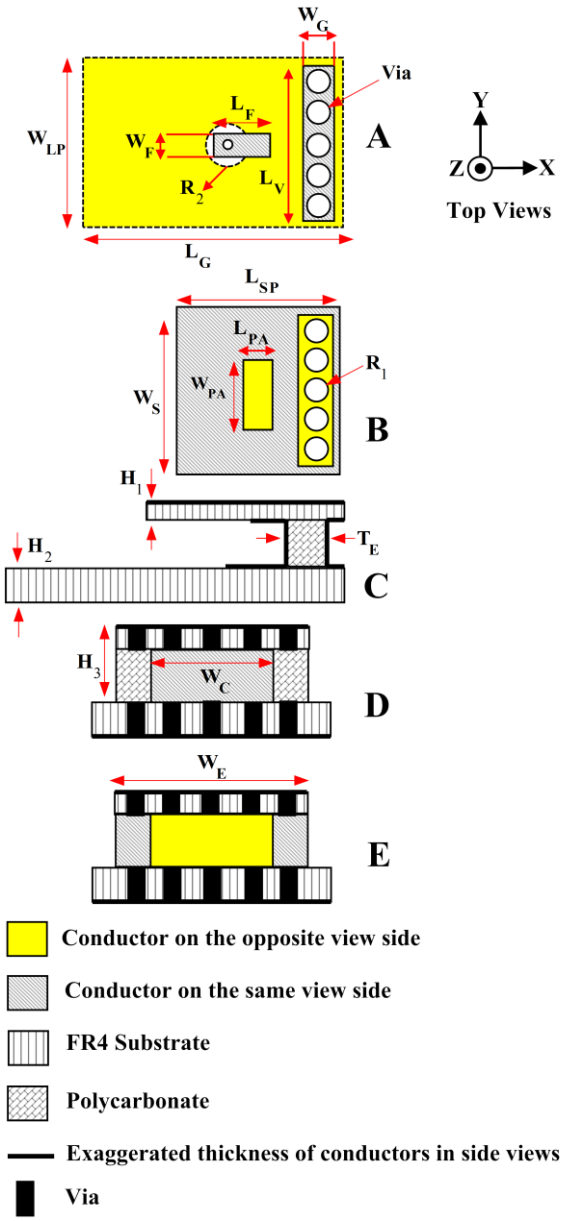

Fig. 1. Schematic of the antenna. A. Top view for sensor substrate, B. Top view for elevated patch. C. Side view, D. Front view, E. Back view.

II. ANTENNA STRUCTURE

The schematic and 3D model of the antenna are depicted in figures 1 and 2 respectively. A is the top view of the main substrate (FR4, 1.6mm, ε_r =4.4, tan δ =0.02) of the wireless sensor which includes a full ground plane in bottom layer and a microstrip feed line on top layer. A large via is made in the middle to connect the microstrip feed line to SMA connector for antenna measurement purposes. The circle cut in the ground plane (radius = R_2) is needed to avoid shorting the SMA center pin to ground. A row of vias were made in the PCB to connect the shorting wall to ground plane of the sensor. B shows the top view of the suspended patch printed on a 1mm FR4 substrate layer and is shorted to ground plane of the sensor through a number of vias and a vertical shorting wall.

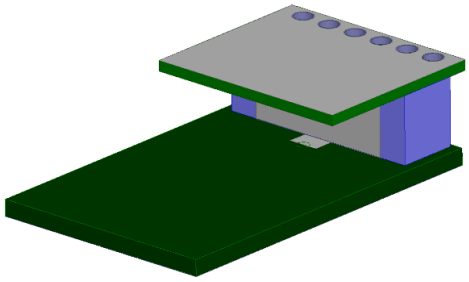

Fig. 2. 3D model of the suspended patch antenna

The vertical shorting wall is printed on side wall of a polycarbonate block using silver ink (see C in Fig.1). C depicts the side view of the antenna that clarifies how the patch is shorted and fed using two printed walls made from ACHESON ELECTRODAG PM-496 conductive silver ink on both sides of a 6mm thick polycarbonate block. Electrical properties of polycarbonate are ε_r =2.5, tan δ =0.01. D and E show the front and back view of the mounted antenna on the sensor respectively. The final optimized value of the parameters shown in Fig.1 are presented in TABLE 1. The coordinate system shown in Fig.1 is related to top view.

TABLE 1. Optimized values of antenna parameters (dimensions in mm)

Parameter	W_G	W_{LP}	W_F	W_{SP}	W_{PA}	W_C	W_E	T_E	R_1
Value	2	20	3	22	12	14.3	22	6	1
Parameter	R_2	H_1	H_2	H_3	L_F	L_V	L_G	L_{PA}	L_{SP}
Value	2.1	1	1.6	7	2	20	1.5	1.5	15.5

III. ANTENNA DESIGN

The dominant mode for a normal rectangular patch is TM_{010} which requires the length of the patch to be half of the wavelength in the resonant frequency of the patch [20]. The length of the shorted suspended patch is half of a normal rectangular patch (L_{SP} in Fig.1) because the shorting wall forces the electric fields to be zero in the shorting point. The lower resonant frequency of the antenna is determined by the length of the shorted patch and is approximately equal to quarter of a wavelength on a FR4 substrate at 2.4 GHz considering the following equation:

$$\lambda_g \approx \frac{c}{f\sqrt{\varepsilon_r}} \qquad (1)$$

λ_g is the wavelength in a medium with the permittivity of ε_r, and f represents the frequency and c is speed of light. The higher resonance of the antenna is affected both by the height of the vertical printed feed ($H_3 - H_1$) and the length of coupling patch (L_{PA} in view B of Fig.1). The length of the suspended patch also influences the higher resonant frequency, because changing the length of the suspended patch alters the capacitive load on the small rectangular feed. As can be seen in Fig.3, after increasing the length of suspended patch greater than a certain length, changing the length of L_{SP} does not affect the higher

resonant frequency anymore because the edge of the suspended patch is far from the feed patch and the capacitive effect between two patches does not change significantly anymore. The parametric study of L_{SP}, L_{PA} and $H_3 - H_1$ shown in figures 3, 4 and 5 explains that the lower resonant frequency is mainly affected by the length of the shorted patch. As shown in Fig.4, increasing the height of the vertical feed decreases the higher resonant frequency because it is part of the inverted L shape feed which is the main current path of this structure. Fig.5 verifies this fact because by increasing the length of the other part of inverted L shape feed (L_{PA}), the upper resonant frequency of antenna decreases.

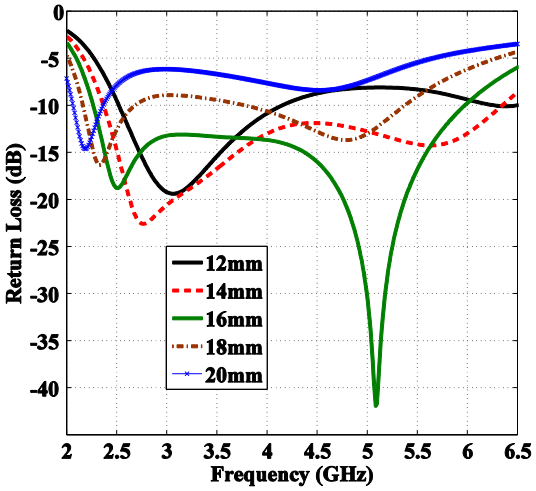

Fig. 3. Parametric study of the length of the shorted patch, L_{SP}

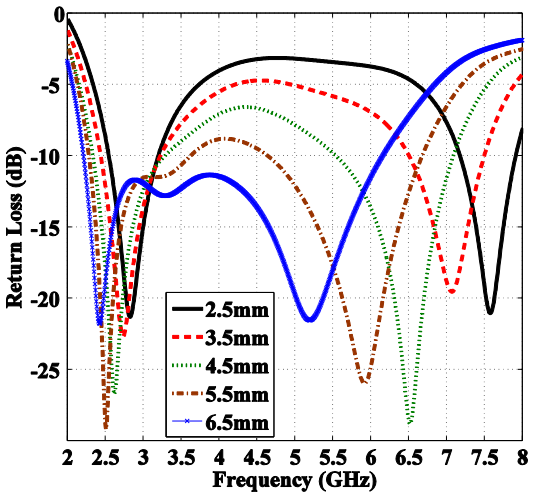

Fig. 4. Parametric study of the height of polycarbonate block ($H_3 - H_1$)

IV. SIMULATION RESULTS

A series of simulation and optimization steps were undertaken using a commercial FEM package [21]. A voxel body model was placed in the distance of 1mm from the ground plane of the sensor in simulation process to investigate the effects of human body on the performance of the antenna. The return loss and total radiation efficiency of the antenna are depicted in Fig.6. The antenna features a wide impedance bandwidth (2.2 GHz – 6.44 GHz) and the total radiation efficiency is better than 90% in the range of 2.5 GHz-6 GHz. The return loss of the antenna does not change considerably after putting the antenna on the body. The radiation pattern of the antenna is presented at three different frequencies in Fig.7. The back lobe of the antenna decreases by increasing the frequency and the directivity increases towards z direction which is desirable for wearable wireless sensors applications. The total radiation efficiency of the antenna decreases less at higher frequencies which is compatible with the more directive radiation patterns in these frequencies.

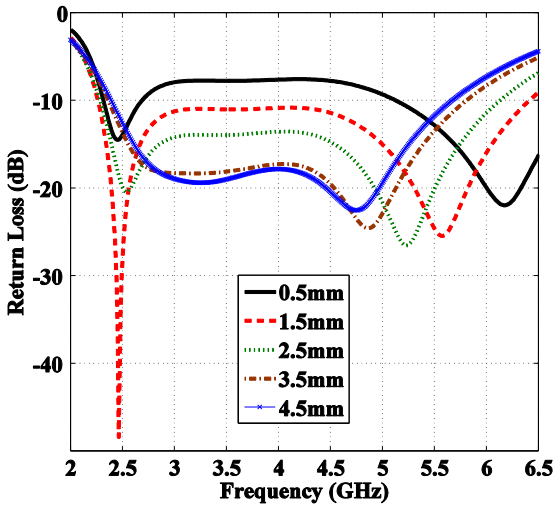

Fig. 5. Parametric study of the length of capacitive feed, L_{PA}

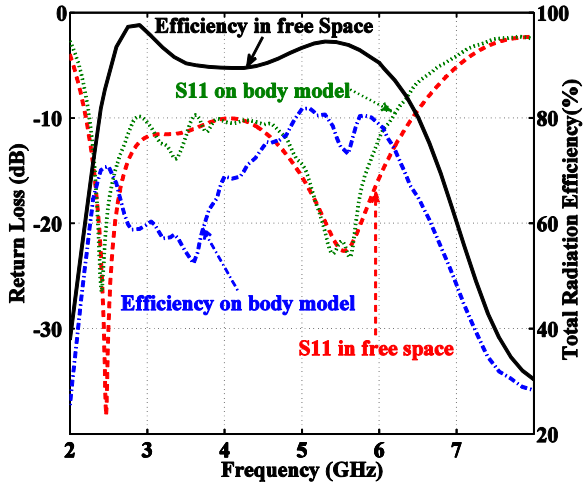

Fig. 6. Simulated return loss and total radiation efficiency of the antenna

V. CONCLUSIONS

A compact, wideband antenna suitable for wearable wireless sensor applications was found to have a 10 dB bandwidth of 98% (2.2 GHz-6.44 GHz). This range covers the needed frequency bands for wireless applications in the range of 2-6 GHz. The radiation pattern is directional and this is a benefit in

the case of wearable applications to reduce the interaction between body tissues and the wireless sensor. The simulated total radiation efficiency of antenna is more than 90% in free space which drops to 70% at 2.4 GHz and 80% at 5.8 GHz when the sensor is located next to a voxel model of the human body.

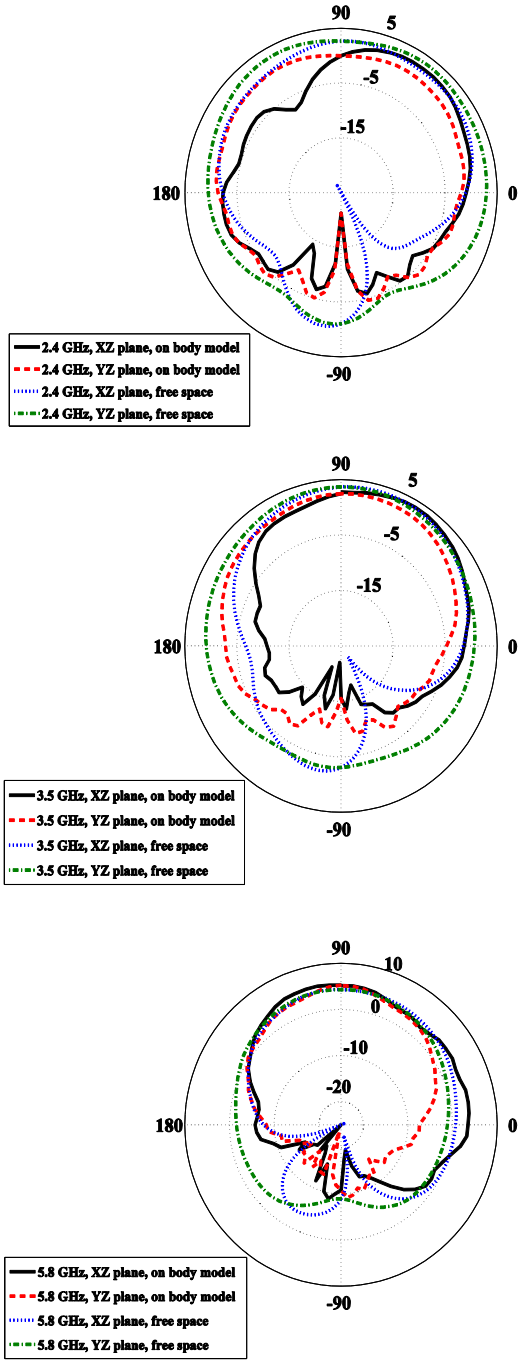

Fig. 7. Radiation patterns (dBi) of the antenna at 2.4 GHz, 3.5 GHz and 5.8 GHz.

REFERENCES

[1] M. V. Varnoosfaderani, D. V. Thiel, and J. Lu, "External Parasitic Elements on Clothing for Improved Performance of Wearable Antennas," *IEEE Sensors Journal,* vol. 15, pp. 307-315, 2015.

[2] T. Kaufmann and C. Fumeaux, "Wearable Textile Half-Mode Substrate-Integrated Cavity Antenna Using Embroidered Vias," *IEEE Antennas and Wireless Propagation Letters,* vol. 12, pp. 805-808, 2013.

[3] S. Z. Zhu and R. Langley, "Dual-Band Wearable Textile Antenna on an EBG Substrate," *IEEE Transactions on Antennas and Propagation,* vol. 57, pp. 926-935, Apr 2009.

[4] P. Salonen, M. Keskilammi, and L. Sydanheimo, "A low-cost 2.45 GHz photonic band-gap patch antenna for wearable systems," *Eleventh International Conference on Antennas and Propagation, Vols 1 and 2,* pp. 719-723, 2001.

[5] D. Gaetano, P. McEvoy, M. Ammann, C. Brannigan, L. Keating, F. Horgan*, et al.*, "Insole Antenna for On-Body Telemetry," *IEEE Transactions on Antennas and Propagation* , vol. PP, pp. 1-1, 2015.

[6] M. Vatankhah Varnoosfaderani, D. Thiel, and J. Lu, "A Wideband Slot Antenna in a Box for Wearable Sensor Nodes," *IEEE Antennas and Wireless Propagation Letters,* vol. PP, pp. 1-1, 2015.

[7] N. Davey, M. Anderson, and D. A. James, "Validation trial of an accelerometer-based sensor platform for swimming," *Sports Technology,* vol. 1, pp. 202-207, 2008.

[8] D. A. James, R. I. Leadbetter, M. R. Neeli, B. J. Burkett, D. V. Thiel, and J. B. Lee, "An integrated swimming monitoring system for the biomechanical analysis of swimming strokes," *Sports Technology,* vol. 4, pp. 141-150, 2011/08/01 2011.

[9] W. K. Toh, C. Zhi Ning, and Q. Xianming, "A Planar UWB Antenna With a Broadband Feeding Structure," *IEEE Transactions on Antennas and Propagation,* vol. 57, pp. 2172-2175, 2009.

[10] K. Cheng-Hung, W. Sung-Jung, and T. Jenn-Hwan, "A Novel Folded UWB Antenna for Wireless Body Area Network," *IEEE Transactions on Antennas and Propagation,* vol. 60, pp. 1139-1142, 2012.

[11] H. T. Chattha, Y. Huang, M. K. Ishfaq, and S. J. Boyes, "Bandwidth enhancement techniques for planar inverted-F antenna," *Microwaves, Antennas & Propagation, IET,* vol. 5, pp. 1872-1879, 2011.

[12] R. Jeen-Sheen, Y. Shih-Huang, and W. Kin-Lu, "A wide-band monopolar plate-patch antenna," *IEEE Transactions on Antennas and Propagation,* vol. 50, pp. 1328-1330, 2002.

[13] H. T. Chattha, Y. Huang, Y. Lu, and X. Zhu, "An ultra-wideband planar inverted-F antenna," *Microwave and Optical Technology Letters,* vol. 52, pp. 2285-2288, 2010.

[14] S. Chan Hwang, H. I. Hraga, R. A. Abd-Alhameed, N. J. McEwan, J. M. Noras, and P. S. Excell, "A Low-Profile Ultra-Wideband Modified Planar Inverted-F Antenna," *IEEE Transactions on Antennas and Propagation, ,* vol. 61, pp. 100-108, 2013.

[15] K. M. Luk, C. L. Mak, Y. L. Chow, and K. F. Lee, "Broadband microstrip patch antenna," *Electronics Letters,* vol. 34, pp. 1442-1443, 1998.

[16] T. S. P. See and C. Zhi Ning, "An Electromagnetically Coupled UWB Plate Antenna,"*IEEE Transactions on Antennas and Propagation, ,* vol. 56, pp. 1476-1479, 2008.

[17] Q. Shi-Wei, R. Cheng-Li, and X. Quan, "A Planar Folded Ultrawideband Antenna With Gap-Loading," *IEEE Transactions on Antennas and Propagation,* vol. 55, pp. 216-220, 2007.

[18] K. Lee, Y. Guo, J. Hawkins, and K. Luk, "Theory and experiment on microstrip patch antennas with shorting walls," *IEE Proceedings-Microwaves, Antennas and Propagation,* vol. 147, pp. 521-525, 2000.

[19] C. R. Rowell and R. D. Murch, "A capacitively loaded PIFA for compact mobile telephone handsets," *IEEE Transactions on Antennas and Propagation,* vol. 45, pp. 837-842, 1997.

[20] C. Balanis, *Antenna Theory: Analysis and Design, 3rd Edition*: Wiley-Interscience, 2005.

[21] "CST Microwave Studio Version, CST.," ed. Framingham, MA, USA, 2012.